Characterization of MLP-Based DGGS Encoders Focused on Data Cubes through Mean Correct Resolution (MCR) Analysis

Israel Nunes da Silva[1], Gabriel Dietzsch[2], Tahisa Neitzel Kuck[2] e Elcio Hideichi Shiguemori[2]
[1]Instituto Tecnológico da Aeronáutica, São José dos Campos/SP - Brasil
[2]Instituto de Estudos Avançados, São José dos Campos/SP - Brasil

***Abstract*— Efficiently mapping coordinates from diverse Coordinate Reference Systems (CRS) to hierarchical Discrete Global Grid System (DGGS) indices is a key challenge for Data Cubes. This study investigates Multilayer Perceptrons (MLPs) for this geocoding task, comparing performance on H3 and rHEALPix grids. As perfect index prediction proved unfeasible for a monolithic MLP, we introduce the Mean Correct Resolution (MCR) metric to measure the average hierarchical depth a model correctly learns. Using a block design, we evaluated the effects of training volume and latitude range, blocking by source CRS (WGS84/Córrego Alegre). The analysis reveals that the rHEALPix grid's regular structure results in a significantly higher MCR than the more complex H3 grid, regardless of the experimental factors. This work provides critical insights into the MLP approach, establishing MCR as an evaluation tool while highlighting its architectural limitations and the higher learnability of rHEALPix for this task.**

***Keywords*— Discrete Global Grid Systems, Neural Networks, Data Cubes.**

I. Introduction

Converting coordinates across various Coordinate Reference Systems (CRS) is a fundamental requirement in geosciences, particularly for uses that integrate multiple geospatial data sources. Most of these transformations, like the Bursa-Wolf or Molodensky transformations, have been extensively formulated in geodetic and cartographic literature [1]. These mathematical models are widely used for projection transformations. However, their formula parameters are not always available or applicable in specific contexts.

While these challenges exist for traditional systems, the growing adoption of Discrete Global Grid Systems (DGGS) introduces a distinct, yet related, transformation problem. DGGS enable the management and analysis of large-scale geospatial data, particularly within the Data Cube paradigm. While DGGS offer significant advantages in data integration and performance, a key operational challenge remains: efficiently and accessibly transforming coordinates from diverse CRS into hierarchical DGGS indices. The native algorithms for this conversion are not always available or computationally efficient, creating a critical interoperability gap. This research investigates a data-driven solution, exploring the viability of Multilayer Perceptrons (MLPs) to learn this complex geocoding transformation directly.

I. N. Silva, israelnunes@ita.br; G. Dietzsch, dietzschgd@fab.mil.br; T. N. Kuck; E. H., Shiguemori, elcioehs@fab.mil.br. This work has been supported by the Brazilian Federal Agency for Support and Evaluation of Graduate Education (CAPES) – Finance Code 001.

In this context, the core objective of this study is to characterize the performance of the AI-based approach. We trained and evaluated MLP models to map coordinates from WGS84 and Córrego Alegre CRSs to H3 and rHEALPix DGGS indices. Recognizing that perfect, bit-for-bit replication of a full hierarchical index is an overly stringent and uninformative binary metric, this study instead focuses on quantifying the practical precision of the models.

To achieve this, we introduce the Mean Correct Resolution (MCR) metric to quantify the average hierarchical depth a model correctly predicts, providing a practical measure of its precision. A formal experimental analysis, structured as a block design, was conducted to assess the main effects of training volume and latitude range, while blocking for the source CRS. The MCR analysis demonstrates that the regular grid structure of rHEALPix is significantly more "learnable"for an MLP, achieving a considerably higher MCR than the more topologically complex H3 grid across all experimental factors. This work offers important insights into the MLP approach for DGGS encoding, reveals its architectural limitations, and establishes MCR as a primary metric for characterizing its actual performance.

II. Background and Related Work

To contextualize the proposed approach and ground the methodology, this section defines the main terms and context of this work, including the theoretical foundations of CRS, DGGS, Data Cubes, and Artificial Neural Networks (ANN). Subsequently, a thorough review of the literature on AI-based geospatial interoperability is carried out, focusing on existing studies of CRS-to-CRS transformations to highlight the uniqueness and contribution of this research.

A. Fundamental Concepts

This work is built upon the intersection of four key concepts: the CRS, which defines the continuous geographic space; the DGGS and the Data Cube, which represent the discrete analysis domain; and the MLP, which serves as the computational engine for the proposed transformation.

1) CRS: A formal framework used to precisely and unambiguously measure and communicate the location of objects in geographic space. As defined by the ISO 19111 standard, a CRS is a coordinate system connected to the Earth through a datum. This datum, comprising a reference ellipsoid and a set of control points, connects the abstract mathematical model to

the physical world. There are map projections that transform the non-Euclidean reference ellipsoid into a Cartesian system, but for this study, we use geographic coordinates of latitude and longitude.

2) DGGS: As defined by the Open Geospatial Consortium [2], under the ISO 19170 series, is a "spatial reference system that uses a hierarchical tessellation of cells to partition and address the globe". It provides a discrete representation of the Earth based on a global grid of geometric cells [3]. Key principles include a hierarchical structure, where cells are consistently subdivided into finer resolutions, and a unique indexing system that allows for efficient spatial queries through algorithmic manipulation rather than expensive geometric calculations. This work focuses on two prominent implementations: H3, based on an icosahedron with hexagonal cells, which prioritizes neighborhood consistency at the cost of area consistency; and rHEALPix (rearranged Hierarchical Equal Area isoLatitude Pixelization), based on a cube with quadrilateral cells, which prioritizes near-perfect area equality, a critical feature for scientific modeling.

3) Data Cube: Simplified from the Earth Observation Data Cube, can be defined as an array of multidimensional data featuring spatial and temporal dimensions, along with derived spectral properties, generated from remote sensing images [4]. These cubes are a response to the massive data volumes from Earth observation. Structuring them with traditional projections introduces significant distortions, and DGGS provide a more robust framework, offering a single, consistent, and hierarchical indexing system for a truly scalable and interoperable Data Cube.

4) ANN: A computational model inspired by biological neural networks. The MLP is a classic ANN architecture composed of an input layer, one or more fully connected hidden layers, and an output layer. It learns complex, non-linear relationships by adjusting its internal parameters (weights and biases) through an optimization algorithm like backpropagation [5].

Ultimately, the operational challenge addressed in this work lies at the intersection of these concepts: leveraging ANN to create a computational bridge between the continuous domain of CRS and the discrete, hierarchical domain of DGGS, to populate Data Cubes with analysis-ready remote sensing data efficiently.

B. Neural Networks in Geospatial Transformations

The application of neural networks has shown significant potential in various geospatial tasks, including spatial pattern recognition, data classification, and coordinate transformations [6]. Specifically within the domain of geodetic interoperability, several studies have successfully employed neural networks as universal function approximators for transformations between traditional Coordinate Reference Systems.

For instance, research by [7], [8], and [9] demonstrated that MLPs can effectively learn the non-linear relationships for local or regional CRS-to-CRS conversions. These studies frame the task as a continuous-to-continuous regression problem, where the network knows the mapping $f : (\phi 1, \lambda 1) \Rightarrow (\phi 2, \lambda 2)$, serving as a robust data-driven alternative when precise transformation parameters are unknown.

However, the problem proposed in this work is fundamentally different. The goal is not to map continuous coordinates to another continuous pair, but to map them to a discrete, structured, and hierarchical DGGS index. This transforms the machine learning problem from regression to one of structured prediction or massively multi-class classification. As such, existing methodologies, including the use of RMSE as a loss function, are not directly applicable. To our knowledge, a systematic characterization of MLP performance for direct CRS-to-DGGS geocoding, particularly in comparing the inherent "learnability"of different DGGS structures, such as H3 and rHEALPix as proposed here, remains an under-explored area of research.

III. Methodology

The methodology to realize the transformation process between CRS and DGGS for Data Cubes using an ANN was structured in four sequential stages: (1) generation of a comprehensive synthetic dataset suitable for training and testing; (2) definition of the core MLP model architecture and its hierarchical training strategy; (3) execution of a rigorous, two-stage hyperparameter optimization process to find the optimal configuration for each model; and (4) implementation of a formal experimental design to assess the final model performance under various conditions using the Mean Correct Resolution (MCR) metric.

A. Data Generation and Pre-processing

To train and evaluate the models, a fully synthetic dataset was generated. Instead of isolated random points, data was created in "image fragments"or patches to simulate the spatial context of remote sensing data, thereby forcing the model to learn the critical decision boundaries between adjacent DGGS cells. The generation process incorporated data augmentation techniques, including random rotation and varying patch sizes from a 3x3 to a 5x5 matrix.

The primary input features are the geographic coordinates of latitude and longitude. These coordinates were pre-processed into a higher-dimensional space using ten frequencies of Fourier Features for each geographic axis. This technique transforms a single coordinate value into a vector of sine and cosine components at multiple frequencies, enabling the MLP to more effectively interpret the fine details and the continuous (for longitude, cyclical) nature of the geographic space. To ensure geographically unbiased training, the sampling of coordinate centers was designed to be uniform by the globe's surface area, eliminating the over-representation of polar regions inherent in a uniform latitude distribution.

B. MLP Architecture and Training Strategy

The MLP was chosen as the neural network architecture because of its proven ability as a universal function approximator (Haykin, 2009). In this logic, the MLP is well-suited for learning complex, non-linear mappings from continuous domains to discrete, hierarchical structures.

The concept of these models is shown in Fig. 1. To address the specific challenges of this task, a specialized architecture was designed:

1) Multi-Head Output: The model features a multi-head architecture. Rather than predicting the entire DGGS index at once, the network has a distinct output head for the base cell and for each subsequent hierarchical digit.

2) Hierarchical Loss Weighting: To guide the training process, we implemented a hierarchical loss weighting strategy. The base cell output head, representing the coarsest and most critical geographic location, was given a weight that decayed inversely with its hierarchical level. This decreasing importance, calculated as 1.5 divided by level, was limited by a floor of 0.1 to ensure that even the finest resolutions maintained a minimal contribution to the total loss function.

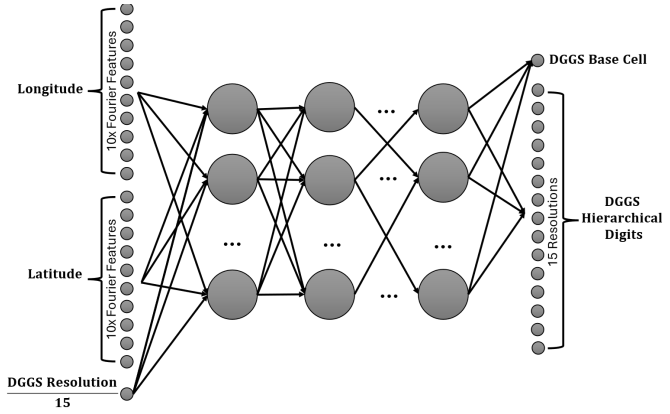

Fig. 1. CRS-to-DGGS MLP Concept.

Four distinct MLP models were trained to manage the specific transformations: H3-WGS84, H3-Córrego Alegre, rHEALPix-WGS84, and rHEALPix-Córrego Alegre. The DGGS (H3 and rHEALPix) were chosen for their fundamentally different geometries, while the CRS (WGS84 and Córrego Alegre) were selected to represent both a global standard and a local datum, simulating a real-world interoperability challenge.

C. Hyperparameter Optimization

A robust hyperparameter configuration for the MLP models was established through a structured two-stage automated optimization process using the Optuna framework, focusing on the WGS84 models as representatives for architecture tuning.

1) Stage 1 (Exploratory Search): An initial broad search (30 trials) was conducted on a 50,000-point dataset to identify promising regions within the hyperparameter space.

2) Stage 2 (Refined Search): Informed by the initial results, a second, more intensive search (50 trials) was conducted on a larger dataset of 100,000 points, using a narrowed search space to fine-tune the configuration.

Each trial in both stages was evaluated using 4-fold stratified cross-validation. Table I summarizes the search space for the initial exploratory stage. The best hyperparameter set found in Stage 2 was used to configure the final models for the experiment.

D. Experimental Design and Statistical Analysis

To formally assess the performance of the final models, we introduced the Mean Correct Resolution (MCR) metric. For each test sample, we identify the maximum resolution level at which the predicted DGGS hierarchy perfectly matches the true hierarchy. The MCR is the arithmetic mean of these values over the entire test set, defined in (1), where MCR is the Mean Correct Resolution, n is the total number of samples in the test set, and $R_{\text{correct}}(i)$ is the Maximum Correct Resolution for sample i.

TABLE I
HYPERPARAMETER SPACE FOR EXPLORATORY SEARCH.

Item	Setting / Range
Cross-validation	4-fold Stratified K-Fold
Epochs per fold	30 (with Early Stopping, patience=5)
Search algorithm	Optuna (30 trials)
Search space:	
Hidden layers	2 – 6
Neurons / layer	{32, 64, 128, 256, 512}
Activation	{relu, tanh, elu}
Optimizer	{adam, rmsprop, sgd}
Learning rate	10^{-5} – 10^{-2} (log-uniform)
Batch size	{32, 64, 128, 256}
Dropout	0.10 – 0.50 (uniform)
L2 regularization	10^{-6} – 10^{-2} (log-uniform)

$$MCR = \frac{1}{n}\sum_{i=1}^{n} R_{\text{correct}}(i) \tag{1}$$

The evaluation was structured as two separate experiments, one for H3 and one for rHEALPix, following a Randomized Complete Block Design (RCBD). This design allows for the analysis of multiple factors while controlling for known sources of variability. The structure for each experiment was as follows:

- **Factors (Variables of Interest):**
  1) **Training Volume** (at 3 levels: 10,000, 100,000, and 1,000,000 data points).
  2) **Latitude Range** (at 3 levels: Equatorial, Mid-latitude, and Polar, based on equal-area zones).
- **Block:** The experiment was blocked by the **Source CRS** (at 2 levels: WGS84 and Córrego Alegre) to isolate its effect, with the hypothesis that its variability would not be significant.

The results were analyzed using a two-factor Analysis of Variance (ANOVA) to determine which factors and interactions had a statistically significant effect on the MCR. A Tukey's Honestly Significant Difference (HSD) post-hoc test was then used for pairwise comparisons between the levels of significant factors. Finally, a diagnostic analysis of the model's residuals, including Q-Q plots, was performed to validate the assumptions of the ANOVA test.

IV. RESULTS AND ANALYSIS

This section presents the empirical results of the study, beginning with the outcomes of the hyperparameter optimization phase, followed by an overview of the final model training, and concluding with a detailed statistical analysis of the formal experiment.

A. Hyperparameter Optimization

The two-stage optimization process successfully identified high-performance hyperparameter configurations for both H3 and rHEALPix models. The initial exploratory search effectively narrowed the vast search space, and the subsequent refined search fine-tuned the configurations on a larger dataset. The optimal parameters found for the final models, trained on 100 thousand data points, are summarized in Table II. Key

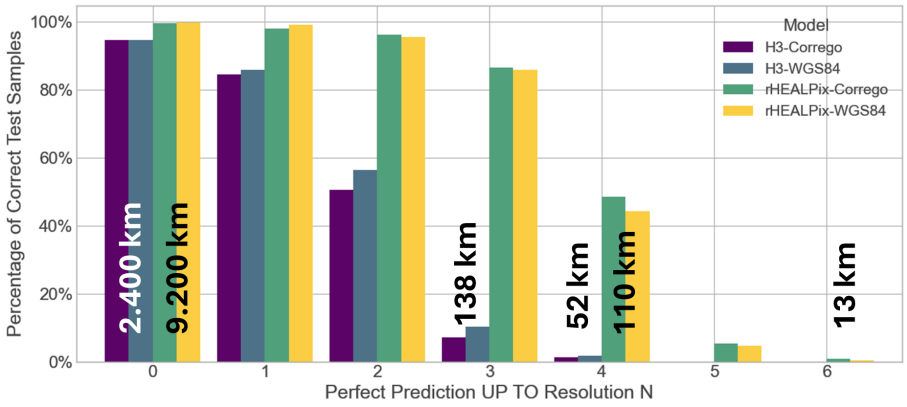

Fig. 2. Cumulative Hierarchical Accuracy by Model. The plot indicates the average cell total length at key resolutions.

findings include convergence on three-layer architectures, the use of the Adam optimizer, and the hyperbolic tangent (tanh) activation function. However, the models differed significantly in their required neuronal capacity and L2 regularization strength, suggesting the varying complexities of the learning tasks.

TABLE II
TRAINING SETTINGS WITH OPTIMIZED HYPERPARAMETERS BY DGGS MODEL.

Item	H3 Setting	rHEALPix Setting
Cross-validation	10-fold Stratified K-Fold	
Epochs per fold	200 (with Early Stopping, patience=15)	
Hidden layers	3	3
Neurons	[512, 512, 1024]	[768, 768, 512]
Activation	tanh	tanh
Optimizer	Adam	Adam
Learning rate	3.26×10^{-4}	5.40×10^{-4}
Batch size	64	64
Dropout	7.36×10^{-3}	2.59×10^{-2}
L2 regularization	9.19×10^{-4}	4.61×10^{-5}

B. Training Results

The final models were trained using the optimal hyperparameters on datasets of varying sizes (10,000, 100,000, and 1,000,000 points). In all cases, the training process demonstrated stable convergence, with loss curves decreasing consistently over epochs. The primary outcome of the training is the model's ability to generalize to unseen data, which is best represented by the cumulative hierarchical accuracy, as shown in Fig. 2. This plot illustrates the percentage of test samples for which each model's prediction was perfect up to a given resolution level. It provides a clear visual summary of the core performance differences between the DGGS models, showing a much steeper decline in accuracy for H3 compared to the more gradual descent for rHEALPix. This performance gap persists even when comparing resolutions of similar physical scale. For instance, at a resolution of approximately 120 km (H3 resolution 3 vs. rHEALPix resolution 4), the H3 model achieves only 8.7% accuracy, while the rHEALPix model reaches 46.5%.

C. Experimental Results

Before conducting any experiment, we analyze the data variation of the factors — training volume and latitude range — using boxplot diagrams, as shown in Fig. 3 and 4. These plots preliminarily indicate that MCR increases geometrically, while volume data increases exponentially, and latitude range causes no effect in H3 models, but have some impact on polar latitudes of rHEALPix.

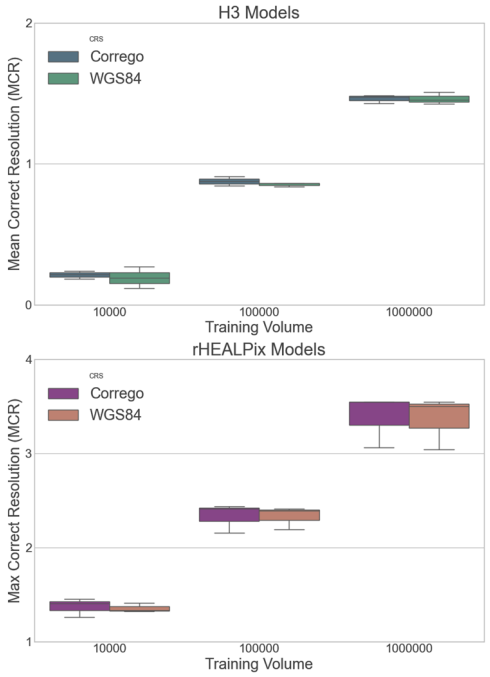

Fig. 3. Distribution of Mean Correct Resolution (MCR) by Training Volume.

The formal experiment was conducted to assess the impact of training volume, latitude range, and source CRS on the MCR. A multi-factor ANOVA was performed separately for each DGGS.

The ANOVA results (Table III) confirm that, as logically expected, for both H3 and rHEALPix, Training Volume is a factor with a highly significant positive effect on MCR ($p < .001$). For the rHEALPix model, the Latitude Range and the interaction between Training Volume and Latitude Range were also found to be statistically significant. The Source CRS, treated as a block, was not significant in either experiment, supporting the hypothesis that its effect is systematic and manageable, given a low MCR.

The Tukey HSD post-hoc tests (Table IV) provide further detail. For both DGGS, each incremental increase in training

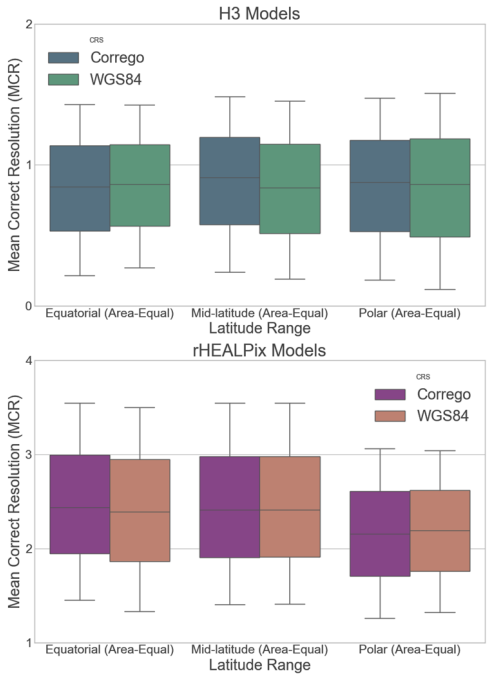

Fig. 4. Distribution of Mean Correct Resolution (MCR) by Latitude Range.

TABLE III
ANOVA TABLE FOR H3 AND RHEALPIX MODELS.

Source	Sum Sq	df	F-value	p-value
H3 Model				
Training Volume	4.76	2	2383.81	$< .001$
Latitude Range	0.00087	2	0.44	0.662
Block (CRS)	0.00088	1	0.88	0.375
Training Volume × Latitude Range	0.0130	4	3.25	0.073
Residual	0.0080	8		
rHEALPix Model				
Training Volume	12.15	2	4209.56	$< .001$
Latitude Range	0.31	2	106.54	$< .001$
Block (CRS)	0.00073	1	0.51	0.496
Training Volume × Latitude Range	0.0967	4	16.76	$< .001$
Residual	0.0100	8		

volume resulted in a statistically significant improvement in the mean MCR. The post-hoc tests for latitude range in the rHEALPix model did not show significant differences between individual pairs, suggesting the effect observed in the ANOVA is complex and distributed across the levels.

Finally, diagnostic checks of the ANOVA residuals were performed. The Q-Q plots, residuals versus fitted values, and histogram of residuals plots (Fig. 5) confirmed that the assumptions of normality were adequately met, thereby validating the statistical analysis. However, the histogram of residuals for the H3 models shows heavier tails, which likely indicates issues in learning the complex geometry, correlating with its lower MCR. Regarding homoscedasticity, the H3 model was acceptable, but rHEALPix showed some tapering in the residuals versus fitted values plot, indicating increasing variability with lower MCR. There are some residual points displaced from the clusters of predicted MCR, which corresponded to the experimental condition combining high training volume with the polar latitude range, a behavior consistent with the significant interaction effect identified by the ANOVA and Tukey test.

TABLE IV
TUKEY HSD POST-HOC TEST FOR THE LATITUDE RANGE FACTOR.

Comparison	Mean Diff.	p-value	Reject
H3 Model			
Equatorial vs. Mid-lat.	0.01	0.9993	False
Equatorial vs. Polar	-0.01	0.9999	False
Mid-lat. vs. Polar	-0.02	0.9986	False
rHEALPix Model			
Equatorial vs. Mid-lat.	0.01	0.9998	False
Equatorial vs. Polar	-0.27	0.8621	False
Mid-lat. vs. Polar	-0.28	0.8528	False

V. DISCUSSIONS

The hyperparameter optimization results suggest that a moderately deep (3-layer) architecture is sufficient, but a high neuronal capacity was needed. The preference for very low dropout rates and the reliance on L2 regularization indicate that weight decay is a more effective regularization strategy for this specific task. Notably, the H3 model required significantly stronger L2 regularization than the rHEALPix model, indicating that the H3 mapping function is more complex and carries a greater risk of overfitting.

From these findings, the statistical analysis confirms that the ”learnability”of diverse DGGS is not uniform. The rHEALPix models consistently achieved a higher MCR than the H3 models across all experimental conditions, even considering approximately the same cell length (resolution 3 of H3 and 4 of rHEALPix). This suggests that the regular, area-equal structure of the rHEALPix grid, based on a cube, presents a smoother and more easily generalizable function for the MLP to approximate. In contrast, the topological complexity of H3, with its 12 pentagonal singularities and greater cell distortion, likely creates a more rugged and complex mapping mathematical function, limiting the depth to which the MLP can accurately learn the hierarchy.

The interaction effects further illuminate this difference in learnability. The significant interaction effect for rHEALPix reveals that increasing training data is particularly beneficial for improving performance in the polar regions, where geometric distortions are most pronounced. For H3, the lack of a latitude effect suggests the model’s difficulty is more uniform across the globe, likely dominated by the inherent complexity of the grid itself. Indeed, the results (Table V) show that each ten-fold increase in training data volume yields an average MCR improvement of approximately 1.0 for rHEALPix. In contrast, for H3, the average improvement is a more modest 0.6.

The primary limitation of this study is the monolithic MLP architecture. The results strongly suggest that a single network trained with a summed loss struggles to learn multiple hierarchical dependencies simultaneously, leading it to prioritize the task with the highest weight (base cell prediction). This is not a failure of the concept, but a revelation of the limits of this specific architecture for this problem.

Despite the inability to achieve perfect index replication, the research demonstrates that the MLP-based approach holds significant practical value. A model that achieves an MCR of approximately 7, as seen with rHEALPix, provides a highly accurate location estimate down to a cell size of a hundred kilometers. For Data Cube applications, enables a fast, parallelizable ”first-pass”geocoding mechanism, ideal for

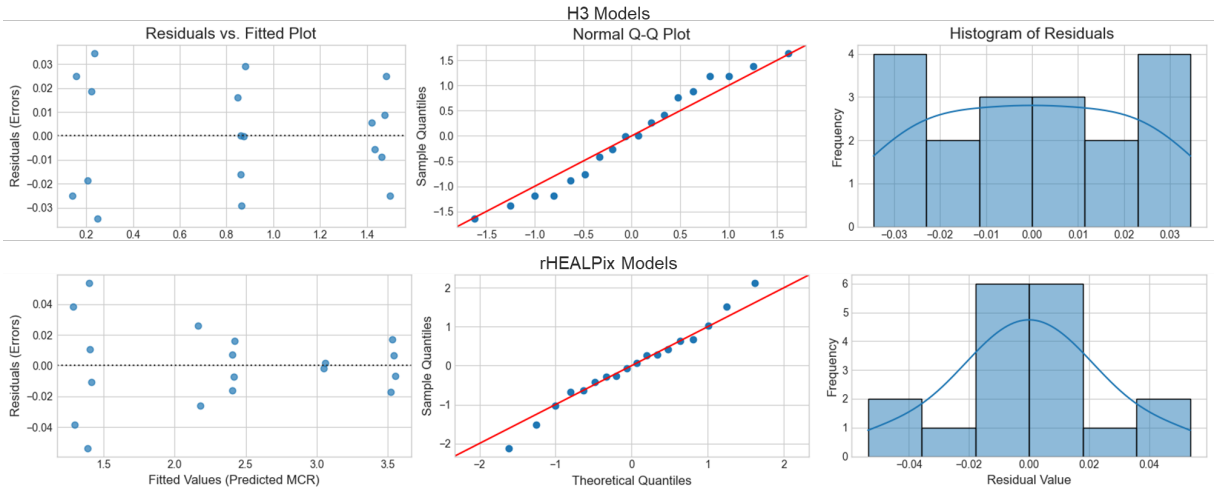

Fig. 5. ANOVA Diagnostic Plots for Each DGGS.

TABLE V
MCR BY DGGS AND TRAINING VOLUME.

DGGS	Training Volume	MCR Mean
H3	10,000	0.2025
	100,000	0.8640
	1,000,000	1.4618
rHEALPix	10,000	1.3635
	100,000	2.3327
	1,000,000	3.3754

rapidly identifying the approximate region of interest for a query or for assigning satellite scenes to coarse-resolution tiles. This AI-driven indexer can serve as an efficient front-end to a traditional, more precise algorithmic system, bridging the gap between raw coordinates and the structured world of DGGS.

VI. CONCLUSIONS

This study aimed to characterize the performance of MLP models in the complex task of transforming geographic coordinates into hierarchical DGGS indices. The comprehensive experimental process, from data generation to statistical analysis, successfully fulfilled this objective, yielding critical insights into the capabilities and limitations of the data-driven approach.

The research's primary discovery is that a monolithic MLP architecture, while proficient at identifying the correct DGGS base cell with high accuracy (94%), is fundamentally inadequate for replicating the whole, deep hierarchy of a DGGS index. The models universally failed to achieve perfect index prediction, a result attributed to the summed loss function causing the network to prioritize the highest-weighted task (base cell prediction) at the expense of learning the finer, sequential details of the hierarchy.

A key comparative finding, enabled by the MCR metric, is that the rHEALPix system demonstrated significantly superior "learnability"compared to H3. The MLP models were able to learn the regular, area-equal structure of the rHEALPix grid to a much greater hierarchical depth, achieving a consistently higher MCR across all experimental conditions. This suggests that the topological complexity and geometric distortions inherent in the H3 grid, including its 12 pentagonal singularities, pose a substantially greater challenge for this type of neural network architecture. For practical Data Cube applications, this means the current models could serve as a "first-pass"geocoder for initial data lookup, rapidly identifying a region of interest at a coarse resolution (approximately 100-300 km), which traditional algorithms could then refine.

The main contributions of this work are threefold: (1) it provides the first systematic characterization and comparison of MLP performance for H3 and rHEALPix geocoding; (2) it introduces and validates the MCR metric as a more informative tool for evaluating hierarchical prediction models; and (3) it formally quantifies, through ANOVA, the significant positive impact of training volume on model performance and the varying effect of latitude on different DGGS structures.

Based on the limitations identified, future work should pivot away from the monolithic architecture. The most promising direction is the investigation of Chained or Cascaded Models, where a sequence of specialist networks is trained, with each model predicting a single level of the hierarchy using the output of the previous level as input. Furthermore, exploring architectures explicitly designed for sequential data, such as Recurrent Neural Networks (RNNs) or Transformers, could yield significant improvements. For lower cell length resolution predictions, even non-deep-learning models like Random Forest could be explored as a simpler, potentially effective alternative.

REFERENCES

[1] R. E. Deakin, "A Note on the Bursa-Wolf and Molodensky-Badekas Transformations," School of Mathematical & Geospatial Sciences, RMIT University, Technical Report, 2006.

[2] R. Gibb, "Topic 21 - Discrete Global Grid Systems - Part 1 Core Reference system and Operations and Equal Area Earth Reference System," pages: 20-040r3. [Online]. Available: https://portal.ogc.org/doi/20-040r3

[3] K. Sahr, D. White, and A. J. Kimerling, "Geodesic Discrete Global Grid Systems," *Cartography and Geographic Information Science*, vol. 30, no. 2, pp. 121–134, Jan. 2003. [Online]. Available: http://www.tandfonline.com/doi/abs/10.1559/152304003100011090

[4] K. R. Ferreira, G. R. Queiroz, R. F. B. Marujo, and R. W. Costa, "BUILDING EARTH OBSERVATION DATA CUBES ON AWS," *The International Archives of the Photogrammetry, Remote Sensing and Spatial Information Sciences*, vol. XLIII-B3-2022, pp. 597–602, May 2022. [Online]. Available: https://isprs-archives.copernicus.org/articles/XLIII-B3-2022/597/2022/

[5] S. S. Haykin, *Neural networks and learning machines*, 3rd ed. New York Munich: Prentice-Hall, 2009.

[6] L. Zhang, L. Zhang, and B. Du, "Deep Learning for Remote Sensing Data: A Technical Tutorial on the State of the Art," *IEEE Geoscience and Remote Sensing Magazine*, vol. 4, no. 2, pp. 22–40, Jun. 2016. [Online]. Available: http://ieeexplore.ieee.org/document/7486259/

[7] A. I. Abbas, O. Y. M. Alhamadani, and M. U. Mohammed, "The application of an artificial neural network for 2D coordinate transformation," *Journal of Intelligent Systems*, vol. 31, no. 1, pp. 739–752, Jul. 2022. [Online]. Available: https://www.degruyter.com/document/doi/10.1515/jisys-2022-0033/html

[8] M. Gullu, M. Yilmaz, I. Yilmaz, and B. Turgut, "Datum Transformation by Artificial Neural Networks for Geographic Information Systems Applications," in *International Symposium on Environmental Protection and Planning: Geographic Information Systems (GIS) and Remote Sensing (RS) Applications Proceedings Book*. Cevre Koruma ve Arastirma Vakfi, 2012, pp. 13–19. [Online]. Available: http://www.cevkorconferences.com/pdf/13-19.pdf

[9] Y. Y. Ziggah, H. Youjian, A. Tierra, A. A. Konaté, and Z. Hui, "Performance evaluation of artificial neural networks for planimetric coordinate transformation—a case study, Ghana," *Arabian Journal of Geosciences*, vol. 9, no. 17, p. 698, Nov. 2016. [Online]. Available: http://link.springer.com/10.1007/s12517-016-2729-7